DOI: 10.18721/JPM.11406
УДК 51-73: 621.574

MODELING OF DYNAMIC PROCESSES IN THE VAPOR COMPRESSION COOLING SYSTEM

D.L. Karelin[1], A.V. Boldyrev[2], V.M. Gureev[3], S.V. Boldyrev[2]

[1] Kazan (Volga region) Federal University, Kazan, Russian Federation;
[2] Kazan Federal University – Naberezhnye Chelny Institute, Naberezhnye Chelny, Russian Federation;
[3] Kazan National Research Technical University named after A. N. Tupolev – KAI, Kazan, Russian Federation

In the paper, a dynamic model of a vapor compression cooling system is presented. In addition to the usual one, it takes into account the working agent's masses in the heat exchangers, this agent's vapor content behavior in time at the outlet of the expansion valve, and the whole spectrum of two-phase flow modes during the working agent's evaporation. It was established that it took more time for temperature's and mass flow's (in a vapor compression cooling system) transitions to steady states than for the rotational speed of the compressor shaft. The connection between the negative dynamics of the evaporation temperature and the initial ambient temperature was shown. Moreover, it was the connection between the delay in stabilization of the mass flow of the working medium and the initial ambient temperature as well as the degree of a pressure increase in the thermodynamic cycle of the vapor compression cooling system.

Keywords: dynamic model, vapor-compression cooling system, heat transfer, temperature difference, compressor

Citation: Karelin D.L., Boldyrev A.V., Gureev V.M., Boldyrev S.V. Modeling of dynamic processes in the vapor compression cooling system, St. Petersburg Polytechnical State University Journal. Physics and Mathematics. 11 (4) (2018) 57–71. DOI: 10.18721/JPM.11406

МОДЕЛИРОВАНИЕ ДИНАМИЧЕСКИХ ПРОЦЕССОВ В ПАРОКОМПРЕССИОННОЙ СИСТЕМЕ ОХЛАЖДЕНИЯ

Д.Л. Карелин[1], А.В. Болдырев[2], В.М. Гуреев[3], С.В. Болдырев[2]

[1] Казанский (Приволжский) федеральный университет, г. Казань, Российская Федерация;
[2] Набережночелнинский институт (филиал) Казанского (Приволжского) федерального университета», г. Набережные Челны, Российская Федерация;
[3] Казанский национальный исследовательский технический университет им. А.Н. Туполева, г. Казань, Российская Федерация

В работе представлена динамическая модель парокомпрессионной системы охлаждения. Особенностями модели являются учет массы рабочего агента в теплообменниках (испарителе и конденсаторе), изменения во времени паросодержания этого агента на выходе из расширительного клапана и учет всего спектра режимов двухфазных течений при испарении рабочего агента. В ходе численного моделирования установлено, что для стабилизации температур и массового расхода в парокомпрессионной системе охлаждения требуется большее время, чем для стабилизации частоты вращения вала компрессора. Показана связь отрицательной динамики температуры испарения с начальной температурой окружающей среды, а также связь задержки стабилизации массового расхода

рабочего агента с указанной начальной температурой и степенью повышения давления в термодинамическом цикле парокомпрессионной системы охлаждения.

Ключевые слова: динамическая модель, парокомпрессионная система охлаждения, теплоотдача, температурный напор, компрессор

Ссылка при цитировании: Карелин Д.Л., Болдырев А.В., Гуреев В.М., Болдырев С.В. Моделирование динамических процессов в парокомпрессионной системе охлаждения // Научно-технические ведомости СПбГПУ. Физико-математические науки. 2018. Т. 11. № 4. С. 61–76. DOI: 10.18721/JPM.11406

Introduction

The current trends in developing energy conversion devices are greatly affected by the problem of maintaining a steady thermal state, complicated by increasing thermal energy density to be dissipated by the cooling system over the entire variation ranges of both the load on the device and the parameters of the external environment. There are currently different methods that can substantially improve the cooling efficiency. One of these methods involves increasing the temperature of the coolant above the boiling point under normal conditions [1, 2] (high-temperature cooling); however the method's considerable drawbacks are, firstly, that it does not solve the problem of cooling efficiency at an ambient temperature significantly exceeding admissible values, and, secondly, it is inapplicable to all systems [3]. A rather effective method for increasing the efficiency of cooling systems and reducing the overall dimensions by improving the heat transport capability of radiators (achieved by changing the functional flow diagram) and a method for heat transmission using the phase transitions in the coolant were proposed in [4]. An azeotropic mixture of water (81.8%) and aniline (18.2%) with a boiling point of 75°C was used instead of classical coolants (water or aqueous solutions of ethylene glycol). It was also noted in this study that alcohols and chlorofluorocarbons (e.g., Freons) might be used as coolants if the issue of high condensation pressures is solved for these compounds.

Modern naval energy systems have high specific power, with large amounts of heat released in a limited volume; effective heat load management in naval electronic systems entails solving problems associated with dissipating this heat [5, 6]. It is established that a separate vapor compression cooling system is needed for stable operation of such systems (for example, electromagnetic railguns, radars, electric motors and motor drives). Special approaches should be taken to designing such systems, since, unlike traditional vapor compression systems operating at steady state, the heat fluxes of the objects cooled in these systems may undergo sharp dynamic changes. In view of the above, vapor compression cooling systems used to control the thermal state should designed based on dynamic models [7].

A static model of a vapor compression cooling system based on theoretical and empirical dependences was described in [8]. The mass flow rate of the cooling fluid, the refrigerating capacity of the evaporator, the power consumption of the compressor and the coefficient of performance were found by the temperatures of the cooling fluid in the evaporator and the condenser, as well as by the degree of superheat of the fluid at the evaporator outlet.

A static mathematical model of a vapor compression cooling system was obtained in [9] by simultaneous solution of the mass balance equations in the compressor and in the heat exchangers, and of the heat balance equations in the condenser and in the evaporator. The heat output was calculated as a function of temperature and mass air flow rate. The parameters of the classical and vapor compression cooling systems were compared with the identical dimensions of heat exchangers and environmental conditions.

Ref. [10] proposed a new method for calculating the condensation temperature taking into account the selected type of cooling fluid, the changes in temperature and mass flow rate of cooling air, and the heat load on the vapor compression cooling system. A procedure for calculating the parameters of the thermodynamic cycle of this system was developed based on this method.

A mathematical model was constructed in [12], and a vapor compression cooling system driven by a gas engine was simulated using the equations of the semi-empirical model of a scroll compressor, the dependence of the power consumption of the gas engine on the compressor

shaft speed, on the ambient air temperature and on the compressor power, and the equations of a model of an evaporator that is a brazed plate heat exchanger.

Notably, the above studies focused on the operating parameters of vapor compression cooling systems in steady state. However, these parameters actually change over time, both during startup and shutdown, and with the changing environmental (or other) factors. Therefore, studying the dynamic characteristics of such systems is important for optimal control of compressor operation, maintaining the required speed, stability and other parameters of vapor compression equipment.

For example, a mathematical model for the dynamics of a vapor compression cooling system based on the laws of conservation of mass and energy in the evaporator, compressor, condenser and expansion valve was given in [13]. Performance characteristics of the system such as the refrigerating capacity and the refrigeration cycle efficiency were analyzed, and different parameters were determined, including the steady-state mass flow rate of the cooling fluid, its degree of superheat in the evaporator. It was found from the time dependences plotted for the rotational speed of the compressor shaft and the mass flow rate of the working agent that the system had a high operational frequency.

An experimental and numerical study on the dynamics of a heat pump operating in cooling mode and equipped with a gas engine driven scroll compressor was carried out in [14]. The mathematical model was represented by energy balance equations, criterial equations of heat transfer for two-phase flows in heat exchangers, and equations for calculating the parameters of the gas engine. The suction and discharge pressures were taken equal to the pressures for evaporation and condensation of the cooling fluid, respectively. Differential equations were solved by the Runge–Kutta method. The time variation of evaporation and condensation temperatures, refrigerating capacity, fuel consumption of the gas engine and power consumption of the compressor shaft were considered.

However, these studies did not consider the variation of the vapor content in the evaporator and the cooling fluid in the heat exchangers with time, which considerably affects the accuracy of the simulation results, since these characteristics can greatly vary during transient processes, for example, in the interval between the time when the system is started and the time when it reaches a steady state. Taking these factors into

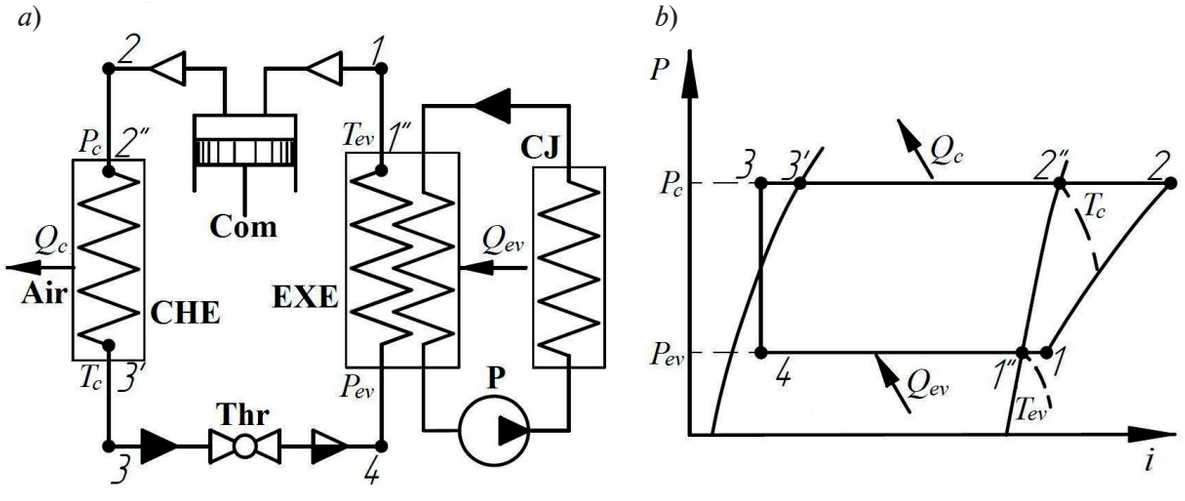

Fig. 1. Circuit diagram of the vapor compression cooling system (*a*) and its thermodynamic cycle *1→2→3→4* (*b*):
Com is the single-stage rotary vane compressor, CHE is the condensing heat exchanger, Thr is the expansion valve, EHE is the evaporating heat exchanger, P is the pump, CJ is the cooling jacket; Air is the air from the fan; T_c, P_c, T_{ev} , P_{ev} are the temperatures and pressures of condensation and evaporation, respectively; Q_{ev} , Q_c are the heating powers of the evaporator and the condenser; $P(i)$ is the thermodynamic diagram of the working fluid (pressure as a function of specific enthalpy for liquid and vapor phases); the dashed lines indicate the isotherms

account should also improve the accuracy of predicting both the heating and cooling times of power units and heat exchangers, as well as other characteristics of transient processes required for designing control units for vapor compression cooling systems.

In this study we have developed a mathematical model of the dynamics of a vapor compression cooling system (Fig. 1). The model is based on solving the equation of a rotary vane compressor and differential equations of a condensing heat exchanger and an evaporating heat exchanger. The model also includes the masses of the working agent contained in the condensing and evaporating heat exchangers, the variation of vapor content with time, and heat transfer during boiling of the working agent in accordance with the diagram for two-phase flow. The model was used to calculate the transient characteristics, in particular, the variation over time of condensation and evaporation (boiling) temperatures and of mass flow rate of the working agent pumped by the compressor.

Construction and operating principles of the vapor compression cooling system

The simulated system operates in a thermodynamic cycle similar to a heat pump and an air conditioner. The system includes a vapor compression circuit *1→2→3→4* (Fig. 1, *b*) that the working fluid (Freon-132b) flows along, containing a single-stage rotary vane compressor (Com), condensing heat exchanger (CHE), expansion valve (adjustable throttle Thr) and evaporating heat exchanger (EHE). Heat is supplied to the evaporator from the cooling circuit including the pump (P), which circulates the coolant (Tosol-65), and the cooling jacket (CJ). The condenser is blown with air from a fan (Air) to dissipate heat.

Dynamic model of the vapor compression cooling system

Assumptions made. We assumed the following in developing a mathematical model describing the dynamics of the vapor compression cooling system:

calculations of the heat transfer coefficient in differential equations of heat balance for heat exchangers did not include the thermal resistances of contaminants and vapor film;

temperature at the interface between the inner wall of the heat exchanger tubes and the vapor film was taken equal to the condensation temperature T_c and evaporation temperature T_{ev}, respectively (see Fig. 1);

mass of the working fluid was calculated using a homogeneous model assuming uniform distribution of vapor and liquid phases and not including the effect of phase slip at the interface;

throttling of the working fluid in the expansion valve was considered to be isenthalpic;

temperatures and mass flow rates of cooled (Tosol-65) and cooling (air) media were taken to be constant;

heat losses to the environment were not taken into account.

Compressor. The specific work l_a of adiabatic compression of the working fluid in the compressor was found by the equation:

$$l_a = P_1 \cdot v_1 \cdot \frac{k}{k-1} \cdot \left[\left(\frac{P_2}{P_1} \right)^{\frac{k-1}{k}} - 1 \right] \qquad (1)$$

where P_1, P_2, Pa, are the pressures at points *1* and *2* of the thermodynamic cycle; v_1, m^3/kg, is the specific volume; k is the polytropic index.

The power N_i consumed by the compressor shaft:

$$N_i = \frac{l_a G_{com}}{\eta_{ad}} \qquad (2)$$

where G_{com}, kg/s, is the mass flow rate of the working fluid (Freon-132b); η_{ad} is the adiabatic efficiency, which was taken equal to 0.82 for the rotary vane compressor [15].

The volumetric flow rate V_{com} (m^3/s) for the vapor drawn into the compressor was calculated (without the vane thickness taken into account) by the following relationship:

$$V_{com} = 2\pi D_{com} l_{com} \varepsilon_{com} n_{com} \lambda_{com}, \qquad (3)$$

where D_{com}, m, is the diameter of the working surface of the compressor housing (cylinder), l_{com}, m, is the length of the rotor (piston); ε_{com}, m, is the displacement of the generator centers of the cylinder and the rotor (eccentricity); n_{com}, s^{-1}, is the number of rotor revolutions per minute; λ_{com} is the flow rate coefficient depending on the degree of pressure increase $\pi_{com} = P_2/P_1$ and the dimensions of the compressor.

Given the admissible load on a vane of a rotary

compressor and depending on the degree of pressure increase π_{com}, we adopted the following relations between the main geometric dimensions of its working elements [15, 16]:

$$\frac{l_{com}}{D_{com}} = 1.8;\ \frac{2 \cdot \varepsilon_{com}}{D_{com}} = 0.140 \quad \text{with } \pi_{com} = P_2 / P_1 \le 2.5; \tag{4}$$

$$\frac{l_{com}}{D_{com}} = 1.8;\ \frac{2 \cdot \varepsilon_{com}}{D_{com}} = 0.115 \quad \text{with } \pi_{com} = P_2 / P_1 \le 5. \tag{5}$$

In this study, we took the degree of pressure increase equal to $\pi_{com} = 4.52$, therefore, taking into account expressions (5) and the ratios for the compressor piston radius $R_{com} = D_{com}/2$ and mass flow rate $G_{com} = V_{com}/v_1$, the mass flow rate equation for a rotary vane compressor takes the form:

$$G_{com}(t) = \frac{1.664 \cdot \pi \cdot R_{com}^3 \cdot \lambda_{com}}{v_1} \cdot n_{com}. \tag{6}$$

The empirical dependence of λ_{com} on the degree of pressure increase π_{com} in Eq. (6) is taken as follows [15]:

$$\lambda_{com} = 1.0 - a \cdot \left(\frac{P_2}{P_1} \right), \tag{7}$$

where $a = 0.05$ and 0.10 for large and for small compressors, respectively.

Equation for the dynamics of evaporation temperature. We considered a multipass shell-and-tube evaporating heat exchanger. The working fluid (Freon-132b) flows inside a tube bundle with Tosol flowing outside it. The heat balance equation for the evaporating heat exchanger has the following form:

$$Q_{ev} = Q_{th.ev} - Q_{com.ev}, \tag{8}$$

where Q_{ev}, W, is the change in enthalpy of the working fluid in the evaporator per unit time; $Q_{th.ev}$, W, is the heat transport power in the evaporator; $Q_{com.ev}$, W, is the heating power carried away by the compressor from the evaporator.

The change in enthalpy of the working fluid in the evaporating heat exchanger per unit time is expressed as

$$Q_{ev} = \frac{Cp'_{ev} + Cp''_{ev}}{2} \cdot m_{ev} \cdot \frac{dT_{ev}}{dt} \tag{9}$$

where Cp'_{ev}, Cp''_{ev}, J/(kg·K), are the isobaric heat capacities of the liquid and gas phases of the working fluid, respectively; m_{ev}, kg, is the mass of the working fluid in the evaporator; T_{ev}, K, is the evaporation temperature of the working fluid in the evaporator; t, s, is time.

The heating power $Q_{com.ev}$, carried away by the compressor from the evaporator:

$$Q_{com.ev} = (i_1 - i_4) G_{com}, \tag{10}$$

where i_1, i_4, J/kg, are the specific enthalpies of the working fluid at the corresponding points of the cycle (see Fig. 1, *b*).

The heat transport power in the evaporator taking into account the logarithmic mean temperature difference (LMTD) takes the following form:

$$Q_{th.ev} = F_{ev} \cdot \frac{1}{\frac{1}{\alpha_{cf.ev}} + \frac{\delta_{p.ev}}{\lambda_m} + \frac{1}{\alpha_{ev}}} \times \times \frac{\left(T'_{cf} - T_{ev}\right) - \left(T''_{cf} - T_{ev}\right)}{\ln\left(\frac{T'_{cf} - T_{ev}}{T''_{cf} - T_{ev}}\right)}. \tag{11}$$

where F_{ev}, m^2, is the heat transfer surface area of the evaporator; $\delta_{p.ev}$, m, is the wall thickness of the evaporator tube; T'_{cf}, T'_{cf}, K, are the cooling fluid (Tosol-65) temperatures at the inlet and outlet of the evaporator, respectively; α_{ev}, W/(m^2·K), is the heat transfer coefficient for boiling of the working fluid in circular tubes; $\alpha_{cf.ev}$, W/(m^2·K), is the heat transfer coefficient of Tosol for a multipass shell-and-tube evaporating heat exchanger; λ_m, W/(m·K), is the thermal conductivity of the material of the wall of the evaporator.

Based on the heat balance equation (8) and the equations for the input and output heating powers (9)–(11), we have obtained the following equation for the dynamics of the evaporation temperature:

$$m_{ev}(t)\cdot\frac{\left(Cp'_{ev}+Cp''_{ev}\right)}{2}\cdot\frac{\mathrm{d}T_{ev}}{\mathrm{d}t}=$$
$$=F_{ev}\cdot\frac{1}{\frac{1}{\alpha_{cf.ev}}+\frac{\delta_{p.ev}}{\lambda_m}+\frac{1}{\alpha_{ev}(t)}}\times$$
$$\times\frac{\left(T'_{cf}-T_{ev}\right)-\left(T''_{cf}-T_{ev}\right)}{ln\left(\frac{T'_{cf}-T_{ev}}{T''_{cf}-T_{ev}}\right)}-(i_1-i_4)\cdot G_{com}(t). \quad (12)$$

The heat transfer coefficient for boiling of the working fluid in circular tubes [22]:

$$\alpha_{ev}(t)=0.28\times10^{-5}\times\frac{\lambda'_{ev}(t)}{d_{ev\_in}}\times$$
$$\times\left(\frac{\upsilon''_{ev}(t)\times d_{ev\_in}}{\nu''_{ev}(t)}\right)^{0.19}\times\left(\frac{\upsilon'_{ev}(t)\times d_{ev\_in}}{\nu'_{ev}(t)}\right)^{0.66} \quad (13)$$
$$\times\left(\frac{\nu'_{ev}(t)}{a'_{ev}(t)}\right)^{0.3}\times\left(\frac{L_{ev}}{d_{ev\_in}}\right)^{1.66}$$

for separated flows (stratified two-phase flow with a smooth and wavy boundary);

$$\alpha_{ev}(t)=0.65\cdot10^{5}\cdot\frac{\lambda'_{ev}(t)}{d_{ev\_in}}\times$$
$$\times\left(\frac{\upsilon''_{ev}(t)\cdot d_{ev\_in}}{\nu''_{ev}(t)}\right)^{0.73}\times\left(\frac{\upsilon'_{ev}(t)\cdot d_{ev\_in}}{\nu'_{ev}(t)}\right)^{-0.73}\times \quad (14)$$
$$\times\left(\frac{\nu'_{ev}(t)}{a'_{ev}(t)}\right)^{0.3}\cdot\left(\frac{L_{ev}}{d_{ev\_in}}\right)^{-1.69}$$

for intermittent flows (slug, annular slug two-phase flow);

$$\alpha_{ev}(t)=0.018\cdot\frac{\lambda'_{ev}(t)}{d_{ev\_in}}\cdot\left(\frac{\upsilon''_{ev}(t)\cdot d_{ev\_in}}{\nu''_{ev}(t)}\right)^{1.19}\times$$
$$\times\left(\frac{\upsilon'_{ev}(t)\cdot d_{ev\_in}}{\nu'_{ev}(t)}\right)^{-0.3}\cdot\left(\frac{\nu'_{ev}(t)}{a'_{ev}(t)}\right)^{0.3} \quad (15)$$

for dispersed flows (dispersed, annular dispersed and annular two-phase flow), where λ'_{ev}, W/(m·K), is the thermal conductivity coefficient of the liquid phase of the working fluid in the evaporator; d_{ev_in}, m, is the internal diameter of the tubes in the evaporator; L_{ev}, m, is the length of the tubes in the evaporator; υ''_{ev}, υ'_{ev}, m/s, are the normalized velocities of, respectively, gas and liquid phases of the working fluid in the evaporator; ν''_{ev}, ν'_{ev}, m^2/s, are the kinematic viscosities of gas and liquid phases of the working fluid in the evaporator; a'_{ev}, m^2/s, is the thermal diffusivity of the liquid phase of the working fluid in the evaporator.

In Eqs. (13)–(15), υ''_{ev}, υ'_{ev} are the normalized velocities of gas and liquid phases of the working fluid, calculated by the following relations:

$$\upsilon''_{ev}(t)=\frac{G_{com}(t)\cdot x_{ev}(t)}{\rho''_{ev}(t)\cdot S_{p.ev}\cdot z_{ev}}; \quad (16)$$

$$\upsilon'_{ev}(t)=\frac{G_{com}(t)\cdot\left(1-x_{ev}(t)\right)}{\rho'_{ev}(t)\cdot S_{p.ev}\cdot z_{ev}}, \quad (17)$$

where z_{ev} is the number of parallel tubes in the evaporator, x_{ev} is the mass vapor content at working point *4* (see Fig. 1, *b*);

$$x_{ev}(t)=\frac{i_4(t)-i'_4(t)}{i''_1(t)-i'_4(t)} \quad (18)$$

where, i''_1, i'_4, J/kg, are the specific enthalpies of the working fluid at the corresponding points of the cycle (see Fig. 1, *b*).

The heat transfer coefficient of Tosol for a multipass shell-and-tube evaporating heat exchanger was determined from the criterial equation for the flow of fluid around a staggered tube bundle [15]:

$$\alpha_{cf.ev}=0.41\cdot\frac{\lambda'_{cf.ev}}{d_{ev.out}}\times$$
$$\times\left(\frac{\upsilon_{cf.ev}\cdot d_{ev.out}}{\nu_{cf.ev}}\right)^{0.6}\cdot\left(\frac{\nu_{cf.ev}}{a_{cf.ev}}\right)^{0.33}, \quad (19)$$

where $\lambda'_{cf.ev}$, W/(m·K), is the thermal conductivity of Tosol in the evaporator; $d_{ev.out}$, m, is the external diameter of the tubes in the evaporator; $\upsilon_{cf.ev}$, m/s, is the maximum velocity of Tosol in the tube bundle in the evaporator's narrowest cross-section; $\nu_{cf.ev}$, m2/s, is the kinematic viscosity of Tosol in the evaporator; $a_{cf.ev}$, m^2/s, is the thermal diffusivity of Tosol in the evaporator.

The outer diameter ($d_{ev.out}$, m) of the streamlined tube in the bundle was taken as the principal dimension in this equation, and the maximum velocity in the bundle in the narrowest cross-section was taken as the principal velocity ($\upsilon_{cf.ev}$, m/s).

Equation for the expansion valve. Upon total condensation, the working fluid passes through the expansion valve, where it expands isenthalpically (process *3→4*, see Fig. 1,*b*) with the pressure decreasing from the condensation pressure P_c to the evaporation pressure P_{ev} as part of the fluid is vaporized.

$$i_3 = i_4 \tag{20}$$

where i_3, i_4, J/g, are the specific enthalpies of the working fluid at the corresponding points of the cycle (see Fig. 1, *b*).

Equation for the dynamics of condensation temperature. In this study we considered a classical condensing heat exchanger, consisting of finned copper tubes with the working fluid (Freon-132b) flowing inside them, and air flowing outside. The heat balance equation for this condenser then has the form:

$$Q_c = Q_{com.c} - Q_{th.c}, \tag{21}$$

where Q_c, W, is the change in enthalpy of the working fluid in the condenser per unit time; $Q_{com.c}$, W, is the heat transport power supplied by the compressor to the condenser; $Q_{th.c}$, W, is the heating power in the condenser.

The change in enthalpy of the working fluid in the condensing heat exchanger per unit time is expressed as

$$Q_c = \frac{Cp'_c + Cp''_c}{2} \cdot m_c \cdot \frac{dT_c}{dt}, \tag{22}$$

where Cp'_c, Cp''_c, J/(kg·K), are the isobaric heat capacities of the liquid and gas phases of the working fluid in the condenser, respectively; m_c, kg, is the mass of the working fluid in the condenser; T_c, K, is the condensation temperature of the working fluid in the condenser.

The heating power supplied by the compressor to the condenser is determined as

$$Q_{com.c} = (i_2 - i_3) G_{com}, \tag{23}$$

where i_2, i_3, J/kg, are the specific enthalpies of the working fluid at the corresponding points of the cycle (see Fig. 1, *b*).

The heat transport power in the condenser taking into account the LMTD takes the following form:

$$Q_{th.c} = F_c \cdot \frac{1}{\frac{1}{\alpha_a} + \frac{\delta_{t.c}}{\lambda_m} + \frac{1}{\alpha_c}} \times \times \frac{\left(T_c - T'_a\right) - \left(T_c - T''_a\right)}{\ln\left(\frac{T_c - T'_a}{T_c - T''_a}\right)}, \tag{24}$$

where F_c, m^2, is the heat transfer surface area of the condenser; $\delta_{t.c}$, m, is the wall thickness of the condenser tube; λ_m, W/(m·K), is the thermal conductivity of the material of the wall of the condenser; T_a, T'_a, K, are the air temperatures at the inlet and outlet of the condenser, respectively; . α_c, W/(m^2·K), is the heat transfer coefficient for condensation of the working fluid in circular tubes; α_a, W/(m^2·K), is the heat transfer coefficient of air in the condenser.

Based on the heat balance equation (21) and the equations for the input and output heating powers (22)–(24), we have obtained the following equation for the dynamics of the condensation temperature:

$$m_c(t) \cdot \frac{\left(Cp'_c + Cp''_c\right)}{2} \cdot \frac{\mathrm{d}T_c}{\mathrm{d}t} = (i_2 - i_3) \cdot G_{com}(t) - -F_c \cdot \frac{1}{\frac{1}{\alpha_a} + \frac{\delta_{t.c}}{\lambda_m} + \frac{1}{\alpha_c(t)}} \cdot \frac{\left(T_c - T'_a\right) - \left(T_c - T''_a\right)}{\ln\left(\frac{T_c - T'_a}{T_c - T''_a}\right)}. \tag{25}$$

To determine the heat transfer coefficient α_f, W/(m^2·K), in the single-phase superheating region *2–2* and supercooling region *3–3* (see Fig. 1, *b*) of the working fluid, we used the criterial equation [15; 18]:

$$\alpha_f(t) = \left(\frac{\lambda_{cf}(t)}{d_{c.in}}\right) \cdot 0.023 \cdot \mathrm{Re}^{0.8}(t) \cdot \mathrm{Pr}^n(t), \tag{26}$$

where n is the exponent for condensation, n = 0.4 [18, 19]; λ_{cf}, W/(m·K), is the thermal conductivity of Freon-132b; $d_{c.in}$, m, is the internal diameter of the condenser tube; Re and Pr are the Reynolds and Prandtl numbers for the cooling fluid flow inside the tube, respectively.

The Reynolds criterion for the cooling fluid

flow inside the tube in Eq. (26) was calculated by the formula:

$$\mathrm{Re} = \frac{4 \cdot G_{com}}{\mu \cdot \pi \cdot d_{c.in}}. \quad (27)$$

The mean value of the heat transfer coefficient α_c during condensation of the working fluid in circular tubes for two-phase region *2′′–3′* (see Fig. 1, *b*) was found, in accordance with [20], from the equation:

$$\alpha_c(t) = \alpha_f(t) \cdot \left(\frac{5}{9} + \frac{2.04}{\mathrm{Pr}^{0.38}(t)} \right), \quad (28)$$

where α_f, W/(m²·K), is the heat transfer coefficient used for calculations by Eq. (26) in the single-phase region.

The heat transfer coefficient α_a for air in the condenser that is a bundle of staggered tubes with external circular fins [21]:

$$\alpha_a = 0.23 \cdot \frac{\lambda_{a\_c}}{b} \cdot \left(\frac{\upsilon_{a\_c} \cdot b}{\nu_{a\_c}} \right)^{0.65} \times \times \left(\frac{b}{d_{c.out}} \right)^{0.54} \cdot \left(\frac{h_{fin}}{b} \right)^{0.14} \cdot \varepsilon_c \cdot \varepsilon_z. \quad (29)$$

where $\varepsilon_c = (S1_c - d_{c.out}/S2_c - d_{c.out})^{0.2}$ is the coefficient; ε_z is the coefficient taking into account the number of vertical rows in the condenser; $S1_c$, $S2_c$, m, are the longitudinal and transverse tube pitches, respectively; $d_{c.out}$, m, is the external diameter of the condenser tube; *b*, m, is the fin pitch; h_{fin}, m, is the fin height; λ_{a_c}, W/(m·K), is the thermal conductivity of air in the condenser; υ_{a_c}, m/s, is the air velocity in the tube bundle in the condenser; ν_{a_c}, m²/s, is the kinematic viscosity of air in the condenser.

Eq. (29) holds true in the range of Reynolds numbers Re_a = 300–22500. The fin pitch *b* is taken as the principal dimension, and the maximum velocity in a narrow cross-section was taken as the principal velocity:

$$\upsilon_{a\_c} = G_a \cdot \left(\rho_a \cdot F_{c.f} \cdot \left(1 - \frac{d_{c.out}}{S1_c} \times \times \left(1 + 2 \cdot \frac{h_{fin}}{b} \cdot \frac{\delta_{fin}}{d_{c.out}} \right) \right) \right)^{-1}, \quad (30)$$

where ρ_a, kg/m³, is the air density; δ_{fin}, m, is the fin height and thickness; $F_{c.f}$, m², is the frontal area of the condenser; G_a, kg/s, is the mass flow rate of air through the condenser.

Mass of the working fluid in the evaporator and condenser. The theoretical mass of the working fluid *m*, kg, in the evaporator and in the condenser, provided that the system is closed, was taken to be constant and determined for nominal operating conditions using the formula:

$$m = m_f + m_v = \frac{V}{\int_0^L dl} \cdot \left[\int_0^L \rho_v \cdot \frac{S_v}{S} dl + \int_0^L \rho_f \cdot \frac{S_f}{S} dl \right], \quad (31)$$

where, m_f, m_v, kg, are the masses of the liquid and gas phases of the working fluid, respectively; *V*, m³, is the internal volume of the tubes; *l*, m, is the longitudinal coordinate; ρ_f, ρ_v, kg/m³, are the densities of the liquid and gas phases of the working fluid, respectively; *S*, m², is the area of the flow cross-section of the tubes; S_f, S_v, m², are the areas of the liquid and gas phases of the working fluid, respectively; *L*, m, is the equivalent length of the tubes (*V*/*S*).

Since the specific volumetric vapor content α′ for the elementary volume is equal to

$$\alpha' = \frac{S_v}{S_v + S_f}, \quad (32)$$

formula (31) can be written in the following form:

$$m = \frac{V}{L} \cdot \left[\int_0^L \left(\rho_v \cdot \alpha' + (1 - \alpha') \cdot \rho_f \right) dl \right] \quad (33)$$

The specific mass vapor content *X* is determined by the ratio of the mass flow rate of the vapor phase $\dot{m}_v$, kg/s, to the total mass flow rate of the cooling fluid $\dot{m}_v + \dot{m}_f$, kg/s:

$$X = \frac{\dot{m}_v}{\dot{m}_v + \dot{m}_f}. \quad (34)$$

Given that $\dot{m} = \rho \cdot S \cdot \upsilon$, the specific volumetric vapor content (32) can be reduced to an equation of the following form:

$$\alpha' = \left[1 + \left(\frac{1 - X}{X}\right) \cdot \frac{\rho_v}{\rho_f} \cdot \gamma\right]^{-1}, \qquad (35)$$

where $\gamma = \upsilon_v/\upsilon_f$ is the coefficient of phase slip at the interface ($\gamma = 1$ for a homogeneous model).

From simultaneous solution of Eqs. (33) and (35) we obtain an expression for calculating the mass m_{ev}, kg, of the working fluid, for example, in the evaporator under nominal operating conditions taking into account the vapor content at working point *4* of the thermodynamic cycle (see Fig. 1, *b*):

$$m_{ev} = \frac{V_{ev}}{L_{ev}} \cdot \int_0^{L_{ev}} \left(\rho_{v.ev} + \frac{\left(\rho_{f.ev} - \rho_{v.ev}\right)}{1 + f_1}\right) dl, \qquad (36)$$

where

$$f_1 = \left[\left(\left(1 - x_{ev}\right) \cdot l / L_{ev} + x_{ev}\right)^{-1} - 1\right] \cdot \left(\rho_{v.ev}/\rho_{f.ev}\right)$$

is the function taking into account the variation in specific mass vapor content X along the length L_{ev} of the evaporator (the vapor content for $l = 0$ is equal to its current value at working point *4*, i.e., $X = x_{ev}$ (see Fig. 1, *b*); the vapor content for $l = L_{ev}$ takes the value $X = 1$); $\rho_{v.ev}$, $\rho_{f.ev}$, kg/m^3, are the densities of the gas and liquid phases of the working fluid in the evaporator; V_{ev}, m^3, is the internal volume of the evaporator tubes.

Accordingly, the expression for calculating the mass m_c, kg, of the working fluid in the condenser assuming that total condensation occurs and the specific mass vapor content varies in the range from 1 to 0:

$$m_c = \frac{V_c}{L_c} \cdot \int_0^{L_c} \left(\rho_{v.c} + \frac{\left(\rho_{f.c} - \rho_{v.c}\right)}{1 + f_2}\right) dl, \qquad (37)$$

where

$$f_2 = \left[\left(1 - l/L_c\right)^{-1} - 1\right] \cdot \left(\rho_{v.c}/\rho_{f.c}\right)$$

is the function taking into account the variation in the vapor content X along the length L_c of the condenser (the vapor content for $l = 0$ is equal to $X = 1$; the vapor content for $l = L_c$ takes the value $X = 0$); L_c, m, is the length of the tubes in the condenser, V_{ev}, m^3, is the internal volume of the condenser tubes, $\rho_{v.c}$, $\rho_{f.c}$, kg/m^3, are the densities of the gas and liquid phases of the working fluid in the condenser.

The variation of the specific mass vapor content X is shown in Fig. 2.

Simulation, results and discussion

Eqs. (12) and (25) for the dynamics of temperatures in the evaporator and condenser (respectively) were solved by the numerical fourth-order Runge–Kutta method with a fixed step. The heat transfer coefficients during evaporation (α_{ev} (13) – (15)) and condensation (α_c (28)) in the two-phase region, as well as the masses of the working

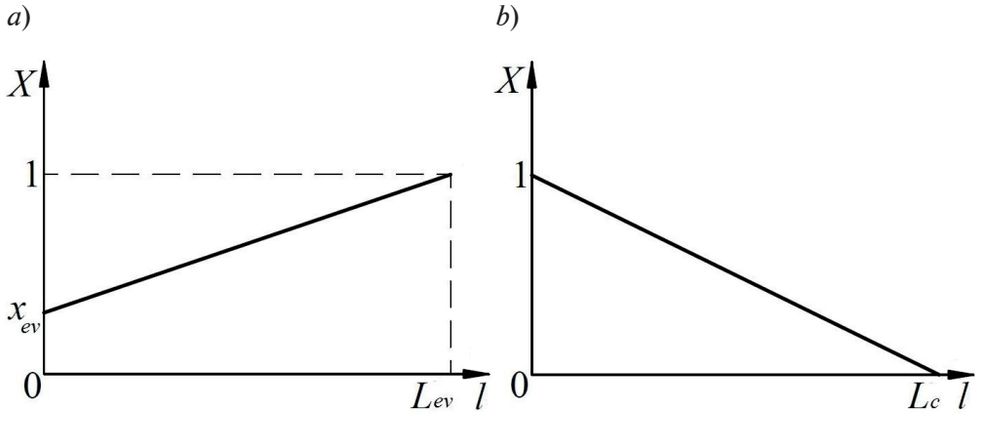

Fig. 2. Variation of specific mass vapor content X: along the length of the evaporating heat exchanger L_{ev} during boiling of the cooling fluid (*a*); along the length of the condensing heat exchanger L_c during condensation of the cooling fluid (*b*); x_{ev} is the mass vapor content at working point *4* of the cycle, l is the longitudinal coordinate

fluid in the evaporator (m_{ev} (36)) and in the condenser (m_c (37)) were functions of the mass flow rate ($G_{com}(t)$ (6)), which, in turn, depended on the rotational speed of the compressor shaft. Acceleration of the compressor shaft when the system was powered up was described by an exponential function (n_s, rpm, is the steady-state value of the rotational speed of the shaft, t_s, min, is the acceleration time of the shaft):

$$n(t) = n_s \cdot \left(1 - \exp\left(\frac{-7 \cdot t}{t_s}\right)\right). \qquad (38)$$

The calculations were performed assuming that at the initial time $t = 0$ the masses of the cooling agent in the condenser ($m_{c.0}$, kg) and in the evaporator ($m_{ev.0}$, kg) are distributed proportional to the internal volumes of these heat exchangers V_c and V_{ev} with the saturated vapor pressure corresponding to the ambient temperature equal to 25°C for the first and 50°C for the second case:

$$m_{c.0} = \frac{m_\Sigma}{V_{ev} + V_c} \cdot V_c; \qquad (39)$$

$$m_{ev.0} = \frac{m_\Sigma}{V_{ev} + V_c} \cdot V_{ev}, \qquad (40)$$

where ($m_\Sigma = m_c + m_{ev}$), kg, is the total mass of the working fluid in heat exchangers (evaporator and condenser) under nominal operating conditions of the vapor compression cooling system.

The heat capacities of the liquid and gas phases (Cp' and Cp'') of the working fluid in the condenser and evaporator, specific enthalpies i at working points of the cycle (see Fig. 1, *b*), thermal conductivities λ, dynamic viscosities μ and densities of the liquid and gas phases (ρ′ and ρ″) were determined at each time as functions of evaporation and condensation temperatures by interpolating the data in reference tables [23].

Based on the results of numerical simulation, we constructed the transient characteristics of the system at startup times from standby mode with ambient temperatures of 25 and 50°C, represented as functions of temperatures of the working fluid in the evaporator and in the condenser and as the corresponding specific volumes of the working fluid (obtained by interpolating data in the tables given in [21]) (Figs. 3–5).

We discovered that the time it took for the evaporation and condensation temperatures (Fig. 3) and the mass flow rate (Fig. 4) to stabilize was rather long, compared to that it took for the compressor shaft to start steadily operating at nominal speed (Fig. 5). For example, the evaporation and condensation temperatures of the working fluid reached a steady-state value in 4.5 s on average, regardless of the ambient temperatures at the moment of system startup (and before it).

A slight decrease in the evaporation temperature of the working fluid was found within 0.1 s after the system was powered up at an ambient temperature of 50°C (see Fig. 3, *b*). The subsequent sharp drop in the evaporation temperature is caused by a change in the two-phase flow from stratified to intermittent (first breakpoint on the characteristic curve). Transition to dispersed flow (the second breakpoint on the curve) was accompanied by a smooth increase in the evaporation temperature up to a steady-state value. According to Eq. (12), negative dynamics of the evaporation temperature is caused by a low heat transfer coefficient due to relatively small logarithmic temperature difference and low normalized velocities υ''_{ev}, υ'_{ev} (see formulae (16) and (17)) of the phases of the working fluid with a significantly larger amount of heat carried away by the compressor.

The temperature difference in the evaporator is considerably increased for the case with the ambient temperature of 25°C, compensating for a small heat transfer coefficient at low normalized velocities of the working fluid. For this reason, the evaporation temperature T_{ev} (see Fig. 3, *a*) increases up to the point in time when the change in the normalized velocities leads changes the character of two-phase flow. The evaporation temperature T_{ev} decreases under intermittent flow and increases smoothly to a steady-state value as dispersed flow establishes in the evaporator tubes.

Analysis of the time variation in the transient characteristics of mass flow rate G_{com} of the cooling fluid (see Fig. 4) and the number of revolutions per unit time n_{com} of the compressor shaft (see Fig. 5) revealed that the flow rate stabilizes more slowly than the rotational speed of the shaft: the delay is 1.2 s at an ambient temperature of 25°C and 0.8 s at 50°C.

Obviously, according to dynamic equations (12) and (25), the heat content of the working fluid in the evaporator and in the condenser, depending on its mass, as well as the heat transfer value, depending on the regime of two-phase flow in the evaporator, influence the stabilization times for the evaporation temperature T_{ev} and the

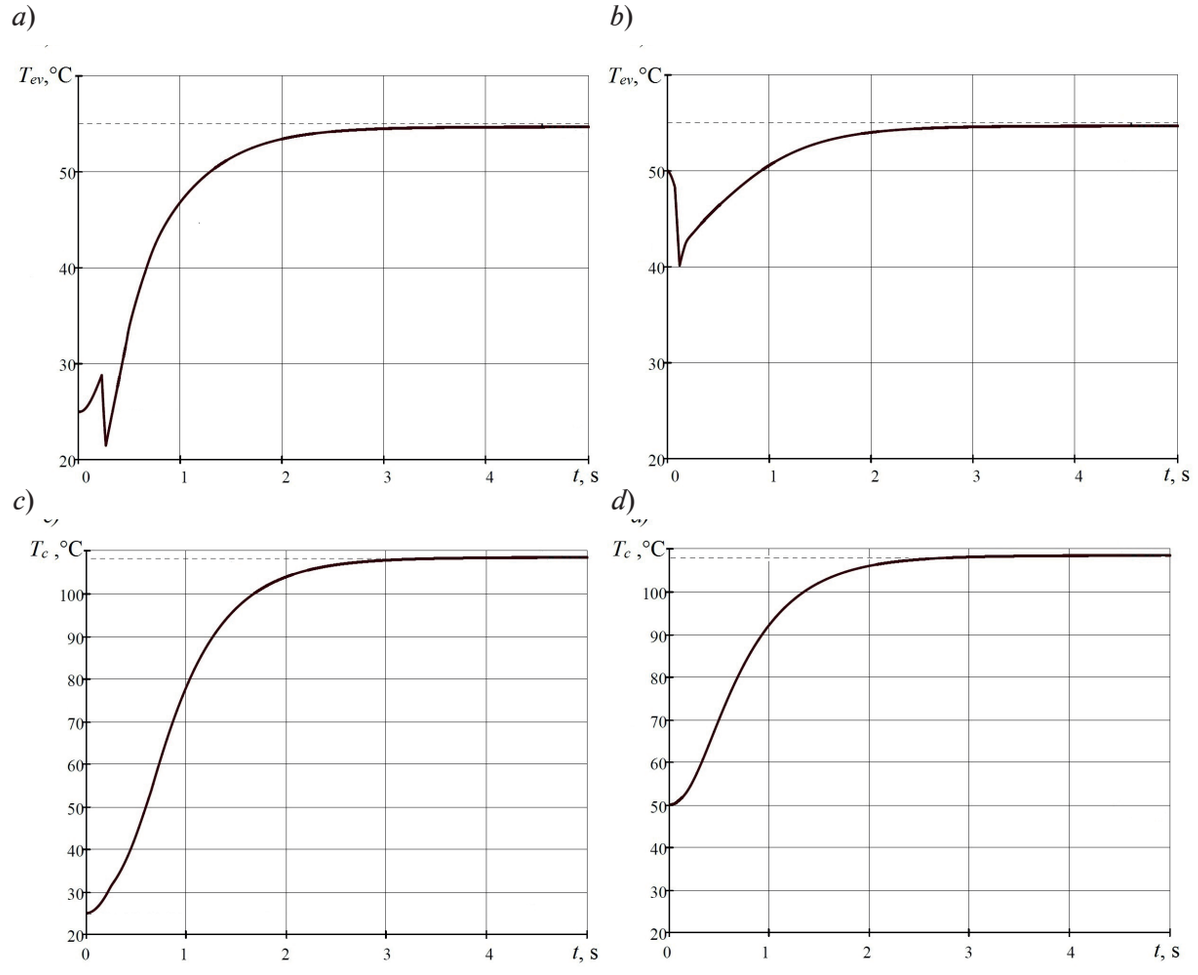

Fig. 3. Transient characteristics of evaporation temperature T_{ev} (*a*, *b*) and condensation temperature T_c (*c*, *d*) at ambient temperatures of 25°C (*a*, *c*) and 50°C (*b*, *d*); the dashed lines indicate the steady-state values of T_{ev} and T_c

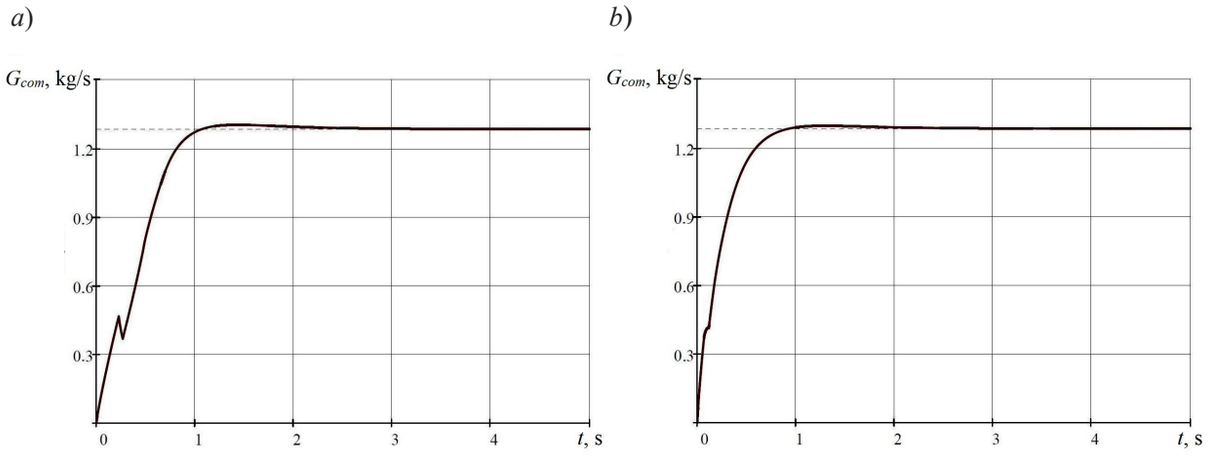

Fig. 4. Transient characteristics of mass flow rate of the working fluid at ambient temperatures of 25°C (*a*) and 50°C (*b*); the dashed lines indicate the steady-state mass flow rates

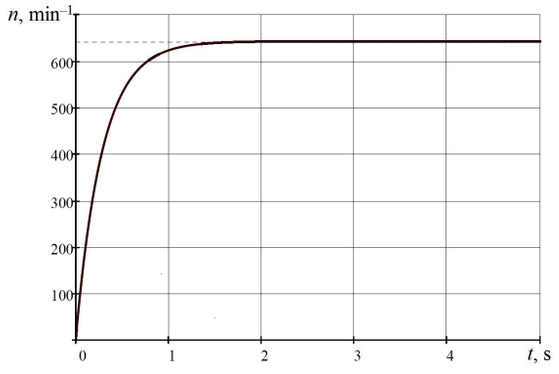

Fig. 5. Dynamics of rotational speed of compressor shaft; the dashed line indicates the steady-state speed

condensation temperature T_c in the vapor compression cooling system.

According to Eq. (5), the increase in the stabilization time of the mass flow rate G_{com} of the compressor is due to the fact that the specific volume of the working fluid at working point *1* (see Fig. 1, *b*) depends on the evaporation temperature T_{ev} and the leakage λ_{com}, whose magnitude increases with increasing pressure π_{com} (6).

Conclusion

In this study, we have developed a dynamic model of a vapor compression cooling system additionally taking into account (by means of criterial equations) the mass of the working fluid in the heat exchangers (evaporator and condenser), the variation over time of the vapor content in the working fluid at point *4* of the thermodynamic cycle at the outlet of the expansion valve, and the entire range of two-phase flows during evaporation of the working fluid. Numerical simulation has revealed that the time it takes for temperatures and mass flow rates to stabilize exceeds that for rotational speed of the compressor shaft in the vapor compression system. The delay depends on the masses of the working fluid in the heat exchangers and on the heat transfer coefficient in the evaporator, which substantially varies depending on the type of two-phase flow. Besides, delayed stabilization of mass flow rate is associated with leaks of the working fluid, which increase proportional to the degree of pressure increase π_{com} and also with the influence of initial conditions of the system, in particular the initial ambient temperature.

The intervals for which a decrease in evaporation temperature was observed with time after the system was powered on from standby mode were found on the transient characteristics. We have established the link between the negative dynamics of the temperature T_{ev} and the initial ambient temperature, and the change in the regime of two-phase flow.

REFERENCES

[1] **N.N. Patrakhaltsev, A.A. Savastenko,** Forsirovaniye dvigateley vnutrennego sgoraniya nadduvom [Boosting internal combustion engines], Legion– Avtodata, Moscow (2004).

[2] **V.G. Krivov, S.A. Sinatov, F.G. Kim, N.A. Ustinov,** Teplootvod v zarubashechnoye prostranstvo forsirovannogo teplovoznogo dizelya pri yego vysokotemperaturnom okhlazhdenii [Heat removal to the volume of the boosted diesel engine with its high-temperature cooling], Dvigatelestroyeniye. (11) (1986) 5–11.

[3] **Eh.I. Sokolovskij, A.I. Ulitenko, T.A. Pyatkina,** Optimizaciya rezhima teplootvoda ot tverdotel'nyh SVCH-priborov v usloviyah povyshennoj temperatury okruzhayushchej sredy // Ehlektronika: Mezhvuz. sb. nauch. trudov. Ryazan', (1978) 128-131.

[4] **Ya.K. Sklifus,** Fazovyye perekhody teplonositelya v sisteme okhlazhdeniya dizelya teplovoza [Phase transitions of the coolant in diesel locomotive cooling system], Proceedings of Rostov State Transport University. (4(29)) (2014) 92–95.

[5] **E. Dilay, J.V.C. Vargas, J.A. Souza, et al.,** A volume element model (VEM) for energy systems engineering, International Journal of Energy Research. 39 (1) (2015) 46–74.

[6] **T.K. Nunes, J.V.C. Vargas, J.C. Ordonez, et al.,** Modeling, simulation and optimization of a vapor compression refrigeration system dynamic and steady state response, Applied Energy. 158 (15) (2015) 540–555.

[7] **J. Catano, T. Zhang, J.T. Wenc, et al.,** Vapor compression refrigeration cycle for electronics cooling, Part I: Dynamic modeling and experimental validation, International Journal of Heat and Mass Transfer. 66 (Nov.) (2013) 911–921.

[8] **R. Cabello, E. Torrella, J. Navarro-Esbri,** Experimental evaluation of the internal heat exchanger influence on a vapor-compression plant performance using R134a, R407C and R22 as working fluids, Applied Thermal Engineering. 24 (13) (2004) 1905–1917.

[9] **D.L. Karelin, V.M. Gureyev, V.L.**

Mulyukin, Modeling system of cooling with two-phase compression installation, Vestnik KGTU im. Tupoleva. (5) (2015) 5–10.

[10] **D.L. Karelin, V.M. Gureyev,** One method of calculation of condensing temperature of the working agent for vapour-liquid compression cooling systems, Vestnik KGTU im. Tupoleva. (4) (2016) 20–24.

[11] **D.L. Karelin,** Metodika rascheta parametrov termodinamicheskogo tsikla parokompressionnoy sistemy okhlazhdeniya [Method for calculating the parameters of the thermodynamic cycle of a vapor compression cooling system]. Trudy Akademenergo. (3) (2017) 23–31.

[12] **E. Elgendy, J. Schmidt, A. Khalil, M. Fatouh,** Modelling and validation of a gas engine heat pump working with R410A for cooling applications, Applied Energy. 88 (11) (2011) 4980–4988.

[13] **Lei Zhao, M. Zaheeruddin,** Dynamic simulation and analysis of a water chiller refrigeration system, Applied Thermal Engineering. 25 (14–15) (2005) 2258–2271.

[14] **S. Sanaye, M. Chahartaghi, H. Asgari,** Dynamic modeling of gas engine driven heat pump system in cooling mode, Energy. 55 (15 June) (2013) 195–208.

[15] **L.M. Rozenfeld, A.G. Tkachev,** Kholodilnyye mashiny i apparaty [Refrigerating machines and devices], GITL, Moscow (1960).

[16] **N.N. Koshkin,** Teplovyye i konstruktivnyye raschety kholodilnykh mashin [Thermal and structural calculations of refrigerating machines], Mashinostroyeniye, Leningrad (1976).

[17] **V.V. Klimenko,** A generalized correlation for two-phase forced flow heat transfer, International Journal of Heat and Mass Transfer. 31 (3) (1988) 541–552.

[18] 2001 ASHRAE handbook, Fundamentals, American Society of Heating, Refrigerating and Air-Conditioning Engineers, Atlanta (2001).

[19] **J.M.S. Jabardo, W.G. Mammani, M.R. Ianella,** Modeling and experimental evaluation of an automotive air conditioning system with a variable capacity compressor, International Journal of Refrigeration. 25 (8) (2002) 1157–1172.

[20] **M.M. Shah,** A general correlation for heat transfer during film condensation in tubes, International Journal of Heat and Mass Transfer. 22 (4) (1974) 547–556.

[21] **V.V. Avchukhov, B.Ya. Payuste,** Zadachnik po protsessam teplomassoobmena [Book of problems in heat and mass transfer processes], Energoatomizdat, Moscow (1986).

[22] **I.G. Chumak, V.P. Chepurnenko, S.G. Chuklin,** Kholodilnyye ustanovki [Refrigeration units], 2nd ed., Legkaya i pishchevaya promyshlennost [Light and Food Industry PH], Moscow (1981).

[23] **B.N. Maksimov, V.G. Barabanov, I.L. Serushkin,** Promyshlennyye ftororganicheskiye produkty [Industrial organofluorine ware], Chemistry PH, Leningrad (1990).

Received 13.05.2018, accepted 02.11.2018.

THE AUTHORS

KARELIN Dmitriy L.
Kazan (Volga region) Federal University
18 Kremlyovskaya St., Kazan, Republic of Tatarstan, 420008, Russian Federation
karelindl@mail.ru

BOLDYREV Alexey V.
Kazan Federal University – Naberezhnye Chelny Institute
68/19 (1/18) Mir Ave., Naberezhnye Chelny, Republic of Tatarstan, 423812, Russian Federation
alexeyboldyrev@mail.ru

GUREEV Viktor M.
Kazan National Research Technical University named after A.N. Tupolev – KAI
10 K. Marx St., Kazan, Republic of Tatarstan, 420111, Russian Federation
viktor.gureev@kai.ru

BOLDYREV Sergey V.
Kazan Federal University – Naberezhnye Chelny Institute
68/19 (1/18) Mir Ave., Naberezhnye Chelny, Republic of Tatarstan, 423812, Russian Federation
underminder@mail.ru

СПИСОК ЛИТЕРАТУРЫ

1. **Патрахальцев Н.Н., Савастенко А.А.** Форсирование двигателей внутреннего сгорания наддувом. М.: Легион–Автодата, 2004. 176 с.
2. **Кривов В.Г., Синатов С.А., Ким Ф.Г., Устинов Н.А.** Теплоотвод в зарубашечное пространство форсированного тепловозного дизеля при его высокотемпературном охлаждении // Двигателестроение. 1986. № 11. С. 5–11.
3. **Соколовский Э.И., Улитенко А.И., Пяткина Т.А.** Оптимизация режима теплоотвода от твердотельных СВЧ-приборов в условиях повышенной температуры окружающей среды // Электроника: Межвуз. сб. науч. трудов. Рязань, 1978. С. 128-131.
4. **Склифус Я.К.** Фазовые переходы теплоносителя в системе охлаждения дизеля тепловоза // Труды Ростовского государственного университета путей сообщения. 2014. № 4 (29). С. 92–95.
5. **Dilay E., Vargas J.V.C., Souza J.A., Ordonez J.C., Yang S., Mariano A.B.** A volume element model (VEM) for energy systems engineering // International Journal of Energy Research. 2015. Vol. 39. No. 1. Pp. 46–74.
6. **Nunes T.K., Vargas J.V.C., Ordonez J.C., Shah D., Martinho L.C.S.** Modeling, simulation and optimization of a vapor compression refrigeration system dynamic and steady state response //Applied Energy. 2015. Vol. 158. No. 15. Pp. 540–555.
7. **Catano J., Zhang T., Wenc J.T., Jensen M.K., Y. Peles Y.** Vapor compression refrigeration cycle for electronics cooling. Part I: Dynamic modeling and experimental validation // International Journal of Heat and Mass Transfer. 2013. Vol. 66. November. Pp. 911–921.
8. **Cabello R., Torrella E., Navarro-Esbri J.** Experimental evaluation of the internal heat exchanger influence on a vapor-compression plant performance using R134a, R407C and R22 as working fluids // Applied Thermal Engineering. 2004. Vol. 24. No. 13. Pp. 1905–1917.
9. **Карелин Д.Л., Гуреев В.М., Мулюкин В.Л.** Моделирование системы охлаждения с парожидкостной компрессионной установкой // Вестник КГТУ им. Туполева. 2015. № 5. С. 5–10.
10. **Карелин Д.Л., Гуреев В.М.** Метод расчета температуры конденсации рабочего агента для парожидкостных компрессионных систем охлаждения // Вестник КГТУ им. Туполева. 2016. № 4. С. 20–24.
11. **Карелин Д.Л.** Методика расчета параметров термодинамического цикла парокомпрессионной системы охлаждения // Труды Академэнерго. 2017. № 3. С. 23–31.
12. **Elgendy E., Schmidt J., Khalil A., Fatouh M.** Modelling and validation of a gas engine heat pump working with R410A for cooling applications // Applied Energy. 2011. Vol. 88. No. 11. Pp. 4980–4988.
13. **Lei Zhao, Zaheeruddin M.** Dynamic simulation and analysis of a water chiller refrigeration system //Applied Thermal Engineering. 2005. Vol. 25. No. 14–15. Pp. 2258–2271.
14. **Sanaye S., Chahartaghi M., Asgari H.** Dynamic modeling of gas engine driven heat pump system in cooling mode // Energy. 2013. Vol. 55. 15 June. Pp. 195–208.
15. **Розенфельд Л.М., Ткачев А.Г.** Холодильные машины и аппараты. М.: ГИТЛ, 1960. 666 с.
16. **Кошкин Н.Н.** Тепловые и конструктивные расчеты холодильных машин. Л.: Машиностроение, 1976. 402 с.
17. **Klimenko V.V.** A generalized correlation for two-phase forced flow heat transfer // International Journal of Heat and Mass Transfer. 1988. Vol. 31. No. 3. Pp. 541–552.
18. 2001 ASHRAE handbook: Fundamentals. Atlanta: American Society of Heating, Refrigerating and Air-Conditioning Engineers, 2001. 544 p.
19. **Jabardo J.M.S., Mammani W.G., Ianella M.R.** Modeling and experimental evaluation of an automotive air conditioning system with a variable capacity compressor // International Journal of Refrigeration. 2002. Vol. 25. No. 8. Pp. 1157–1172.
20. **Shah M.M.** A general correlation for heat transfer during film condensation in tubes // International Journal of Heat and Mass Transfer. 1974. Vol. 22. No. 4. Pp. 547–556.
21. **Авчухов В.В., Паюсте Б.Я.** Задачник по процессам тепломассообмена. М.: Энергоатомиздат, 1986. 144 с.
22. **Чумак И.Г., Чепурненко В.П., Чуклин С.Г.** Холодильные установки. 2-е изд., перераб. и доп. М.: Легкая и пищевая промышленность, 1981. 344 с.
23. **Максимов Б.Н., Барабанов В.Г., Серушкин И.Л.** Промышленные фторорганические продукты. Ленинград: Химия, 1990. 464 с.

Статья поступила в редакцию 13.05.2018, принята к публикации 02.11.2018.

СВЕДЕНИЯ ОБ АВТОРАХ

КАРЕЛИН Дмитрий Леонидович – *кандидат технических наук, доцент кафедры высокоэнергетических процессов и агрегатов Казанского (Приволжского) федерального университета.*
420008, Российская Федерация, Республика Татарстан, г. Казань, Кремлевская ул.,18
karelindl@mail.ru

БОЛДЫРЕВ Алексей Владимирович – *кандидат технических наук, доцент кафедры высокоэнергетических процессов и агрегатов Казанского (Приволжского) федерального университета.*
423812, Российская Федерация, Республика Татарстан, г. Набережные Челны, пр. Мира, 68/19 (1/18).
alexeyboldyrev@mail.ru

ГУРЕЕВ Виктор Михайлович – *доктор технических наук, заведующий кафедрой теплоэнергетики и энергетического машиностроения Казанского национального исследовательского технического университета им. А.Н. Туполева – КАИ.*
420111, Российская Федерация, Республика Татарстан, г. Казань, ул. К. Маркса, 10.
viktor.gureev@kai.ru

БОЛДЫРЕВ Сергей Владимирович – *кандидат технических наук, доцент кафедры высокоэнергетических процессов и агрегатов Казанского (Приволжского) федерального университета.*
423812, Российская Федерация, Республика Татарстан, г. Набережные Челны, пр. Мира, 68/19 (1/18).
underminder@mail.ru